Ultralight Biomass-derived Carbon Fibre Aerogels for Electromagnetic and Acoustic Noise Mitigation

Yi Hou[1#], Jing Quan[2#], Ba Quoc Thai[1], Yijing Zhao[2], Xiaoling Lan[2], Xiang Yu[3], Wei Zhai[2], Yong Yang[1]*, and Boo Cheong Khoo[2]

[1] National University of Singapore, 117411, Singapore

[2] Department of Mechanical Engineering, National University of Singapore, 9 Engineering Drive 1, 117575, Singapore

[2] Institute of High Performance Computing, A*STAR, 138632, Singapore

*Corresponding author. E-mail: tslyayo@nus.edu.sg

[#]These authors contributed to the work equllly and should be regarded as co-first authors

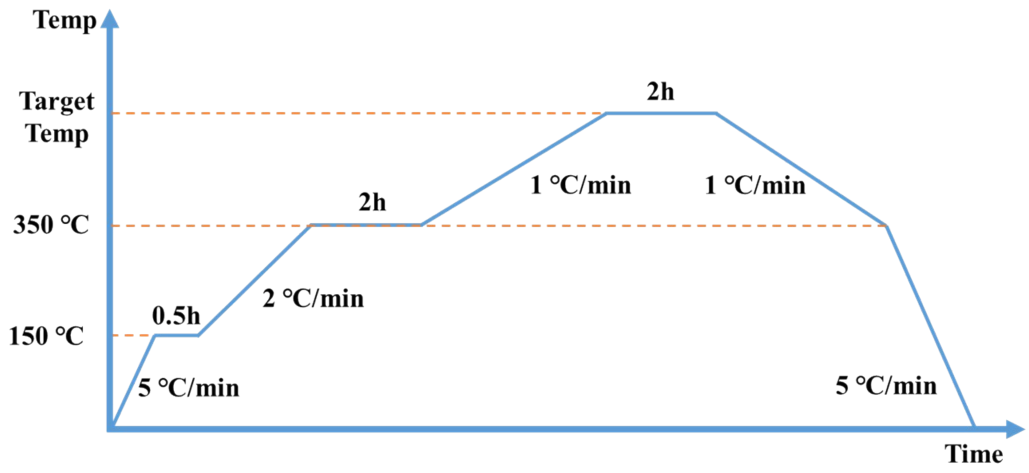

Fig. S1. Heating program for the carbonization process of SA

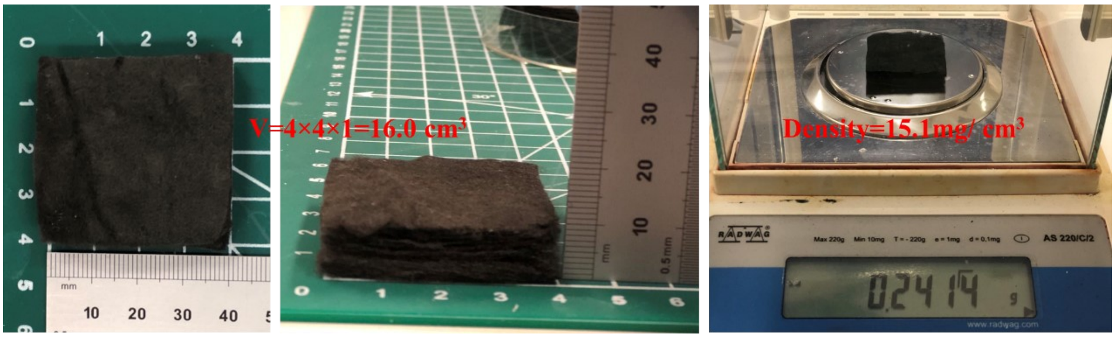

Fig. S2 Illustration of the weight and volume measurement for SA-670 sample.

Table S1. Comparison of density for silk fibres, SA-650/670/700/1500.

Sample	Silk	SA-650	SA-670	SA-700	SA-1500
Density/(mg/cm^3)	18.5	14.7	15.1	15.4	11.8

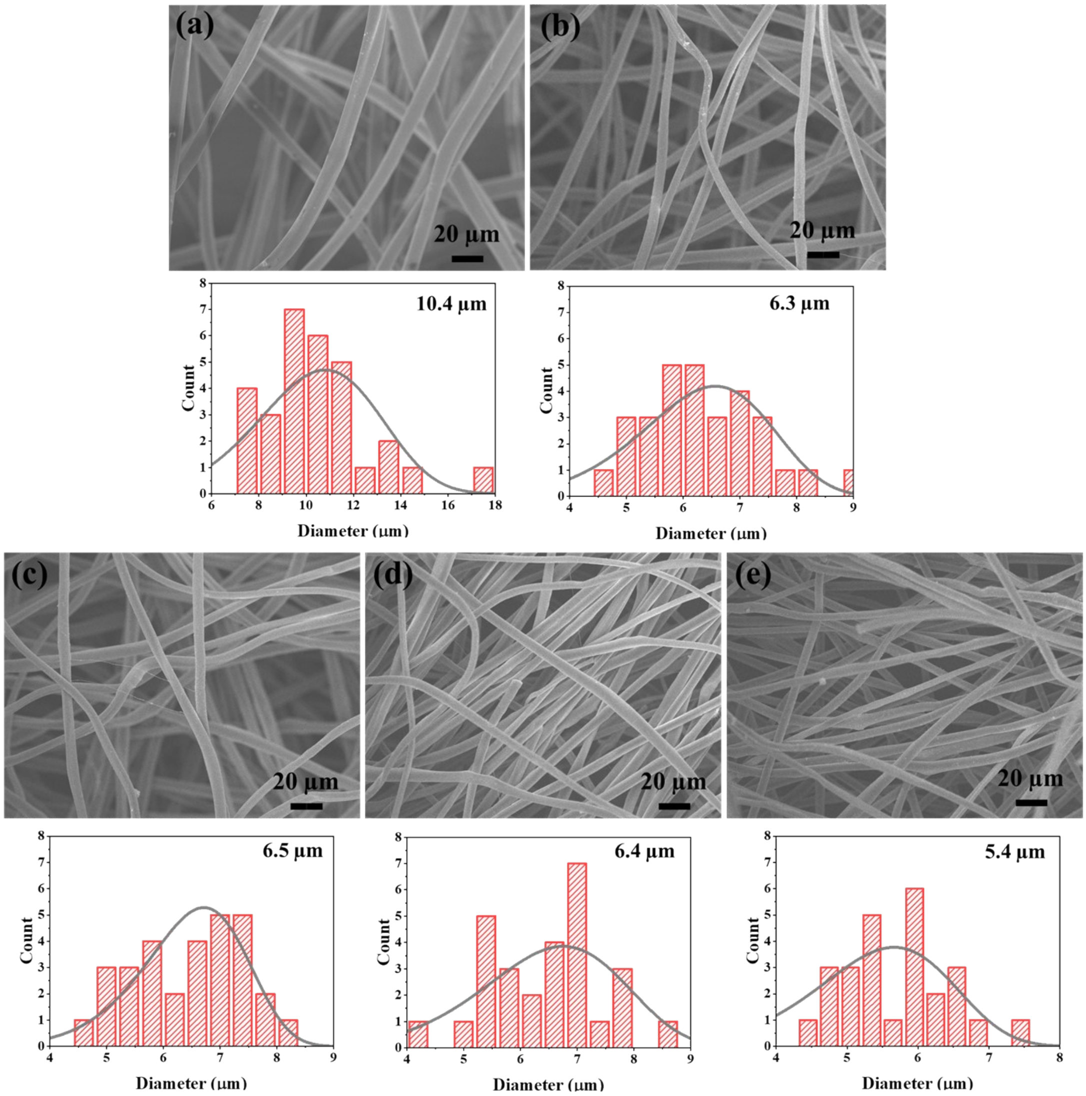

Fig. S3. SEM images and the fibre size distribution of (a) silk fibres, (b) SA-650, (c) SA-670, (d) SA-700 and (e) SA-1500

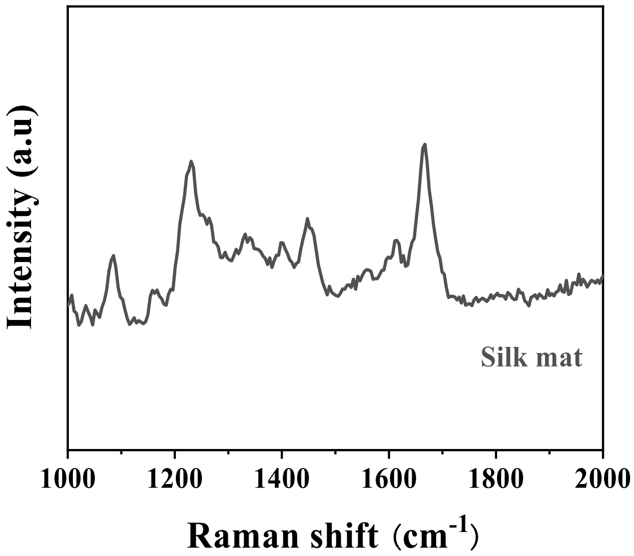

Fig. S4. Raman spectrum of degummed silk fibres

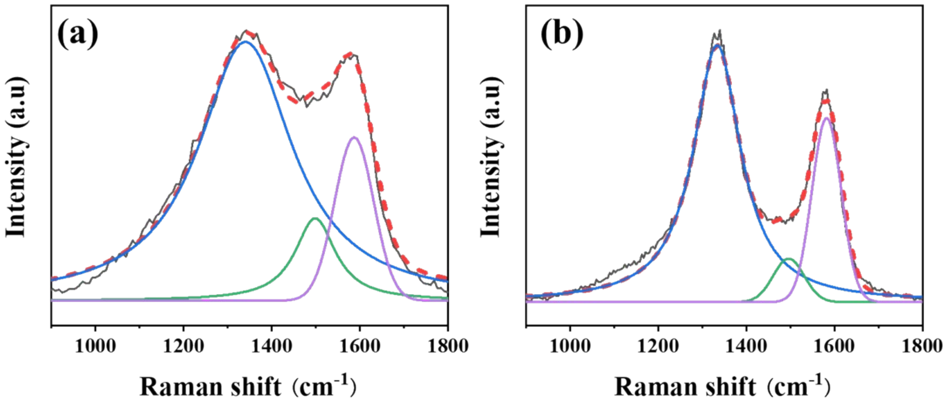

Fig. S5. Mixed Gaussian–Lorentzian fitting for D and G bands of Raman spectra for (a) SA-670 and (b) SA-1500

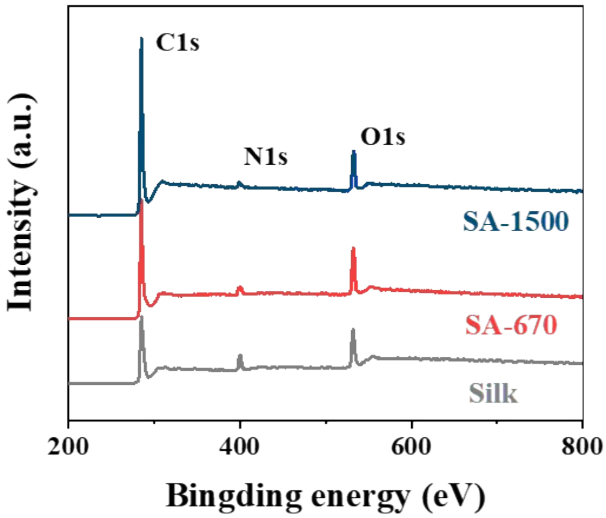

Fig. S6. Comparison of XPS survey spectra for degummed silk fibres, SA-670 and SA-1500.

Table S2. Comparison of element contents obtained from XPS analysis for degummed silk fibres, SA-670 and SA-1500.

Sample	C at%	O at%	N at%
Silk	73.7	16.9	9.4
SA-670	77.5	15.0	7.4
SA-1500	86.9	10.2	2.9

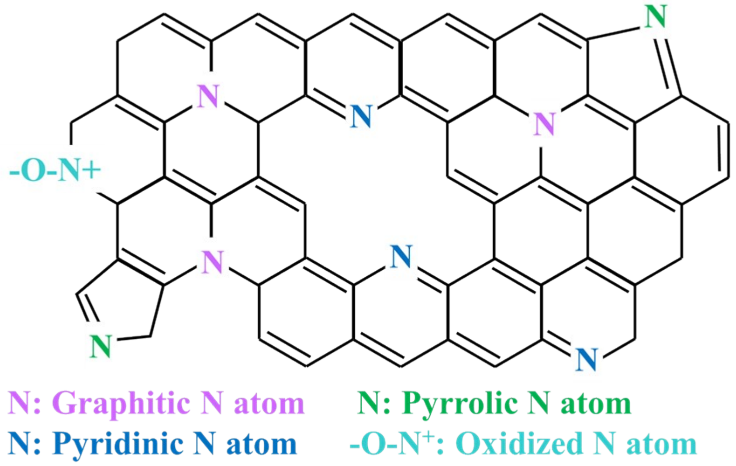

Fig. S7. Schematic diagram of N-doped graphene with graphitic N, pyrrolic N, pyridinic N and oxidized N atoms.

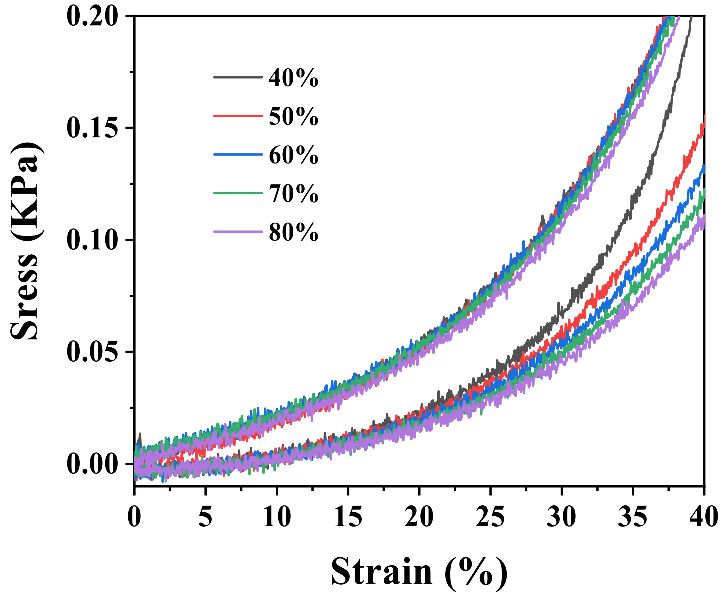

Fig. S8. Stress-strain curves of SA-670 with set strains from 40% to 80% (Partially enlarged view)

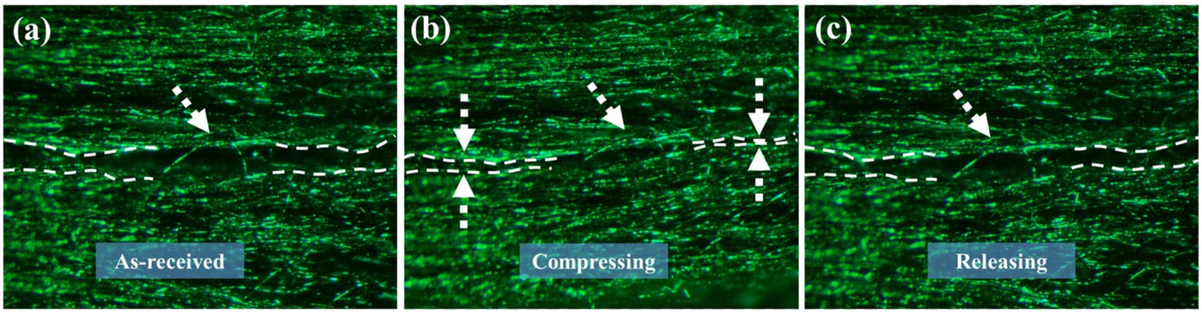

Fig. S9. Cross-section morphology changes of SA-670 during a compressing-releasing cycle.

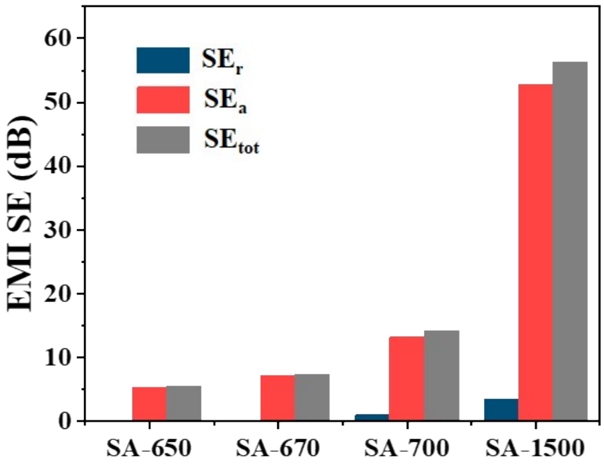

Fig. S10. Average EMI SE_r, SE_a and SE_{tot} of SA samples with different annealing temperatures.

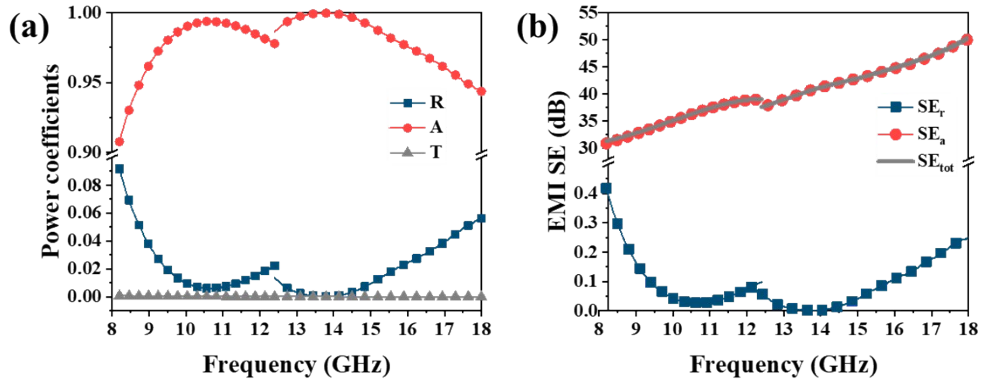

Fig. S11. Frequency dependent: (a) power coefficients and (b) EMI shielding effectiveness (SE_r/SE_a/SE_{tot}) of SA-670/1500 in X+Ku band

Table S3 Comparison of EMI shielding performance for some reported materials

Type	Materials	A /dB	R /dB	A/(A+R)	EAB(A>0.9)/ GHz	Testing Frequency GHz	Density mg/cm^3	ref
		EMI shielding properties (average values)						
CNT	VMQ/Fe_3O_4@MWCNT/ Ag@NWF composite foams	0.427	0.573	0.427	0.8(7.6-8.4)	2-18	380	[1]
	VMQ/MWCNTs/Fe_3O_4 nanocomposite foam	~0.650	~0.350	0.650	0	8.2-12.4	320	[2]
	MWCNT/graphene WPU/Textile composite textile film	0.735	0.265	0.735	0	8.2-12.4	~1000	[3]
	VMQ/Ag@GF/MWCNT/Fe_3O_4 composite foams	0.820	0.180	0.820	0.2(8.2-8.5)	2-18	500-1500	[4]
	TPU/CNT composite	0.50	0.500	0.500	0	8.2-12.4	1200	[5]
rGO	rGO@Fe3O4/T-ZnO/Ag/WPU film	0.610	~0.390	0.610	0.7(9.8-10.5)	8.2-12.4	~1500	[6]
	EBAg/FeCo@rGO/ WPU composite foam	0.920	0.080	0.920	1.8(8.2-10)	8.2-12.4	~3500	[7]
	PDMS/rGO/SWCNT nanocomposite	0.780	0.220	0.780	0	8.2-12.4	~1200	[8]
	rGO/Carbon/polyurethane aerogel	0.590	0.410	0.590	0	8.2-12.4	100	[9]
	CCA@rGO/PDMS composite	0.320	0.680	0.320	0	8.2-12.4	~1200	[10]
C nanofiber	Co/C@CNF-900 aerogel	~0.800	~0.200	~0.800	0	8.2-12.4	1.74	[11]
	CNF/AgNW@Fe_3O_4 composite sponges	0.600	0.400	0.600	0	8.2-12.4	170	[12]
MXene	Polymer/MXene composite foams	0.945	0.0500	0.950	2.77(5.4-8.17)	5.38-8.17	~300	[13]
	MXene(Ti3C2Tx)/ANFs hybrid aerogels	0.0856	0.914	0.0856	0	8.2-12.4	84.0	[14]

	MXene aerogel	0.910	0.090	0.910	4.2(8.2-12.4)	8.2-12.4	62.6	[15]
Metal	Laminated Al film w/ η-gradient film	0.990	0.00960	0.990	8.5(1.5-10)	1.5-10	~270	[16]
	$BiFeO_3$/ $BaFe_7(MnTi)_{2.5}O_{19}$ composite	~0.625	~0.300	~0.676	0	8.2-12.4	~8000	[17]
	EP/NCCF/ACET foam	0.590	0.410	0.590	0	8.2-12.4	210	[18]
	TPU/CIP/Ni mesh composite	0.630	0.370	0.630	0	18-26.5	~1500	[19]
SA	SA-670/1500 Average	0.979	0.02086	0.979	9.8(8.2-18)	8.2-18	15.1	ours
	SA-670/1500 Peak	0.9998	0.000149	0.99985				

Table S4 Comparison of sound absorption performance for some reported materials

Materials	NRC	Density(mg/cm^3)	Thickness(mm)	ref
PAN/PVB-PET nanofiber aerogel	0.41	10.76	20	[20]
SiO_2/rGO nanofiber sponge	0.56	9.33	30	[21]
$Y_2Zr_2O_7$ flexible fibrous membrane	0.60	44	30	[22]
Kenaf fibers	0.50	50	60	[23]
Hemp fibers	0.39	50	30	[23]
Coconut fibers	0.49	60	50	[23]
Cane bark	0.45	145	40	[23]
GO-melamine foam	0.58	24.12	26	[24]
PU/textile waste foam	0.59	65	40	[25]
SiO_2 particle aerogel	0.48	80-85	30	[26]
Coir fibers	0.48	153	30	[27]
SA-670	0.60	15.1	30	ours

Supplementary Methods

1 Calculation of EMI shielding effectiveness

According to the Calculation theory of shielding effectiveness, when the incident EM wave is transformed at the surface of a material, the incident power could be divided into the reflected power, absorbed power and transmitted power, which could be represented by the power coefficient R (reflectivity), A (absorptivity) and T (transmissivity). The electromagnetic interference shielding effectiveness (EMI SE_{tot}, SE_a and SE_r) were calculated by measured S parameters (S_{11}, S_{22}, S_{12} and S_{21}) with the following equations:[28]

$$SE_{tot} = 10log_{10}\left(\frac{P_i}{P_t}\right) = 10log_{10}\left(\frac{1}{T}\right) = SE_r + SE_a \quad \text{(S1)}$$

$$SE_r = 10log_{10}\left(\frac{P_i}{P_{AV}}\right) = 10log_{10}\left(\frac{1}{1-R}\right) \quad \text{(S2)}$$

$$SE_a = 10log_{10}\left(\frac{P_{AV}}{P_t}\right) = 10log_{10}\left(\frac{1-R}{T}\right) \quad \text{(S3)}$$

$$SE_{tot} = SE_r + SE_a \quad \text{(S4)}$$

$$R = |S_{11}|^2 = |S_{22}|^2 \quad \text{(S5)}$$

$$T = |S_{12}|^2 = |S_{21}|^2 \quad \text{(S6)}$$

where SE_{tot}, SE_a and SE_r mean the total, absorption and reflection efficiency. P_i and P_t mean the power of incident and transmitted EM waves, and available power (P_{AV}=P_i-P_t) refers to the net power entering the material.

2 Sound absorption performance simulation of fibrous materials

The sound absorption coefficient α is given by:

$$\alpha = 1 - |R|^2 \tag{S7}$$

in which the sound pressure reflection coefficient R is given by:

$$R = \frac{Z_s - \rho_0 c}{Z_s + \rho_0 c} \tag{S8}$$

Where Z_s is the surface impedance and $\rho_0 c$ represents the characteristic impedance of air. For a single layer absorber with the depth of d under a rigid back, the Z_s could be given by:

$$Z_s = - jZ_c \cot(k_c d) \tag{S9}$$

Where Z_c and k_c are the characteristic impedance and complex wave number of the absorber. Based on the empirical models developed by the work of Delany and Bazley,[27, 29] Z_s and k_c of highly porous and homogeneous sound absorbers could be given by:

$$Z_c = \rho_0 c\left(1 + 0.0571\left(\frac{\rho_0 f}{\sigma}\right)^{-0.754} - j0.087\left(\frac{\rho_0 f}{\sigma}\right)^{-0.732}\right) \tag{S10}$$

$$k_c = \omega/c\left(1 + 0.0978\left(\frac{\rho_0 f}{\sigma}\right)^{-0.7} - j0.189\left(\frac{\rho_0 f}{\sigma}\right)^{-0.595}\right) \tag{S11}$$

where ρ_0 is the air density (~ 1.21 kg/cm^3), $\omega = 2\pi f$ is the angular frequency. For the fibrous absorbers with the fibre diameter ranging from 6 to 10 μm, the flow resistivity σ could be given by the following relationship[30]:

$$\sigma = \frac{10.56\eta(1 - \varepsilon)^{1.531}}{a^2 \varepsilon^3} \tag{S12}$$

where η is the viscosity of air (1.84×10^{-5} Pa s), a is the diameter of fibres and ε is the porosity of the absorber.

References

1. J. Yang, X. Liao, G. Wang, J. Chen, W. Tang, T. Wang and G. Li, *J. Mater. Chem. C.*, 2020, **8**, 147-157.
2. J. Yang, X. Liao, J. Li, G. He, Y. Zhang, W. Tang, G. Wang and G. Li, *Compos. Sci. Technol.*, 2019, **181**, 107670.
3. M. Dai, Y. Zhai and Y. Zhang, *Chem. Eng. J.*, 2021, **421**, 127749.
4. J. Yang, X. Liao, G. Wang, J. Chen, P. Song, W. Tang, F. Guo, F. Liu and G. Li, *Compos. Sci. Technol.*, 2021, **206**, 108663.
5. D. Feng, D. Xu, Q. Wang and P. Liu, *J. Mater. Chem. C*, 2019, **7**, 7938-7946.
6. Y. Xu, Y. Yang, D.-X. Yan, H. Duan, G. Zhao and Y. Liu, *ACS Appl. Mater. Interfaces*, 2018, **10**, 19143-19152.
7. H. Duan, H. Zhu, J. Gao, D.-X. Yan, K. Dai, Y. Yang, G. Zhao, Y. Liu and Z.-M. Li, *J. Mater. Chem. A*, 2020, **8**, 9146-9159.
8. S. Zhao, Y. Yan, A. Gao, S. Zhao, J. Cui and G. Zhang, *ACS Appl. Mater. Interfaces*, 2018, **10**, 26723-26732.
9. X.-X. Wang, J.-C. Shu, W.-Q. Cao, M. Zhang, J. Yuan and M.-S. Cao, *Chem. Eng. J.*, 2019, **369**, 1068-1077.
10. P. Song, B. Liu, C. Liang, K. Ruan, H. Qiu, Z. Ma, Y. Guo and J. Gu, *Nano-micro lett.*, 2021, **13**, 1-17.
11. Y. Fei, M. Liang, L. Yan, Y. Chen and H. Zou, *Chem. Eng. J.*, 2020, **392**, 124815.
12. Y. Chen, H. Luo, H. Guo, K. Liu, C. Mei, Y. Li, G. Duan, S. He, J. Han and J. Zheng, *Carbohydr. Polym.*, 2021, 118799.
13. X. Jia, B. Shen, L. Zhang and W. Zheng, *Carbon*, 2021, **173**, 932-940.
14. Z. Lu, F. Jia, L. Zhuo, D. Ning, K. Gao and F. Xie, *Compos. Part B: Eng.*, 2021, **217**, 108853.
15. R. Bian, G. He, W. Zhi, S. Xiang, T. Wang and D. Cai, *J. Mater. Chem. C*, 2019, **7**, 474-478.
16. T. Kim, H. W. Do, K.-J. Choi, S. Kim, M. Lee, T. Kim, B.-K. Yu, J. Cheon, B.-w. Min and W. Shim, *Nano Letters*, 2021, **21**, 1132-1140.
17. Y. Li, H. Yang, X. Hao, N. Sun, J. Du and M. Cao, *J. Alloy. Compd.*, 2019, **772**, 99-104.
18. H. Duan, H. Zhu, J. Yang, J. Gao, Y. Yang, L. Xu, G. Zhao and Y. Liu, *Compos. Part. A: Appl. S.*, 2019, **118**, 41-48.
19. S. H. Ryu, Y. K. Han, S. J. Kwon, T. Kim, B. M. Jung, S.-B. Lee and B. Park, *Chem. Eng. J.*, 2022, **428**, 131167.
20. L. Cao, Y. Si, Y. Wu, X. Wang, J. Yu and B. Ding, *Nanoscacle*, 2019, **11**, 2289-2298.
21. D. Zong, L. Cao, X. Yin, Y. Si, S. Zhang, J. Yu and B. Ding, *Nat. Communications*, 2021, **12**, 6599.

22. Y. Xie, L. Wang, Y. Peng, D. Ma, L. Zhu, G. Zhang and X. Wang, *Chem. Eng. J.* 2021, **416**, 128994.
23. U. Berardi and G. Iannace, *Appl. Acoust.*, 2017, **115**, 131-138.
24. M. J. Nine, M. Ayub, A. C. Zander, D. N. Tran, B. S. Cazzolato and D. Losic, *Adv. Funct. Mater.*, 2017, **27**, 1703820.
25. A.-E. Tiuc, H. Vermeşan, T. Gabor and O. Vasile, *Energy Procedia*, 2016, **85**, 559-565.
26. C. Buratti, F. Merli and E. Moretti, *Energ. Buildings*, 2017, **152**, 472-482.
27. M. Hosseini Fouladi, M. Ayub and M. Jailani Mohd Nor, *Appl. Acoust.*, 2011, **72**, 35-42.
28. M. Peng and F. Qin, *J. Appl. Phys.*, 2021, **130**, 225108.
29. M. Delany and E. Bazley, *Appl. Acoust.*, 1970, **3**, 105-116.
30. F. P. Mechel., *Formulas of acoustics*, Springer, New York, 2002.